

AD-A056 435

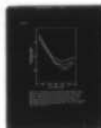
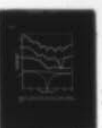
ARMY MISSILE RESEARCH AND DEVELOPMENT COMMAND REDSTO--ETC F/G 20/3
MIE THEORY FOR NON SPHERICAL PARTICLES, (U)
JUN 78 B W FOWLER

UNCLASSIFIED

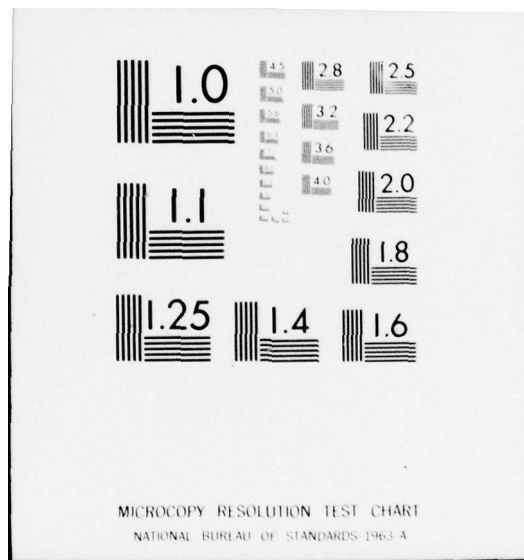
NL

1 of 1

AD
A056 435



END
DATE
FILMED
8 -78
DDC



AD A056435

JDC FILE COPY

FOWLER

LEVEL II

①

11 JUN 1978

12 15p

⑥ Mie Theory for Non Spherical Particles

⑩ Bruce W. Fowler, PhD.
USAMIRADCOM

Redstone Arsenal, AL 35809

DDC
RECEIVED
JUL 10 1978

D

I. INTRODUCTION

This work was motivated during a study of radiative transfer through aerosols¹ when it was realized that spherical aerosol cross sections and phase functions only could be provided by Mie theory. Because many aerosols are irregular in shape, another formalism is needed to provide the optical parameters needed for radiative transfer calculations. The literature of previous efforts on the scattering of electromagnetic waves from irregular particles is extensive², although many of these calculations were directed either to various approximate approaches or to the problem of conducting materials only. An example of both these limitations is the application of least-squares³ techniques to match electric fields at the surface of a conductor. How the least-squares solution is related⁴⁻⁶ to the boundary conditions is unclear.

Several recent efforts⁴⁻⁶ using integral equation formulations deserve special attention since not only are the boundary conditions properly accounted for, but numerical results are presented. References (4) and (5) are based on the scalar rather than the vector wave equation. Reference (6) is completely general, but was only applied to conducting particles. Another entirely different effort of note⁷ which will be addressed later was that of Chylek, Grams and Pinnick (hereafter Chylek et al.) Chylek et al. modify the Mie theory to account for particle irregularity on the empirical grounds that the phase functions of irregular particles do not exhibit glories. As a result, they modify the resonance behavior of the field expansion coefficients to model irregular particle behavior. Chylek et al. have presented calculations that enjoyed better agreement with experimental data than did Mie theory.

78 06 12 028

DISTRIBUTION STATEMENT A

Approved for public release;
Distribution Unlimited

393 169

1

JOB

FWLER

In this paper, the scattering of a plane electromagnetic wave by an irregular but cylindrically symmetric dielectric particle is solved by generalizing the original work of Mie.^{8,9} As in the original work, the expansion coefficients of the scattered and interior (to the dielectric particle) electric and magnetic fields are obtained by satisfying the boundary conditions. Because of the particle irregularity, the expansion coefficients are coupled and form a set of linear equations that must be solved numerically. Both the integral and differential equation approaches are equivalent in analogy to the calculation of the scattering amplitude in quantum mechanics by solving either the Schrodinger or the Lippman-Schwinger equation.¹⁰ Further, both approaches develop into solutions of linear algebraic equations.

It must be emphasized that both References (4)-(6) and this paper are limited in applicability to "slightly" irregular particles whose deviation from a smooth geometric shape is much less than the wavelength. This limitation on solving the scattering problem for "arbitrary" irregular particles is reviewed by Millar.² In essence the limitation arises from the fact that the scattered field solutions incorporate radial functions that become outgoing spherical wave representations in the far field, but not functions that represent scattering of light from one area on the surface of the particle to another area. Consequently, the problem of multiple scattering between areas on the particle have to be neglected. While the overall problem may be handled by dividing the particle into subparticles¹¹ and satisfying the boundary conditions for and between all particles, this paper will be limited to only "slightly" irregular particles.

The differential equation approach is, of course, also valid for "slightly" irregular particles without cylindrical symmetry, but these calculations require more computer core space than is commonly available. In Section II of this paper, the Mie solution for a spherical particle is reviewed by developing the differential equation formalism. Section III is an extension of this formalism to cylindrically symmetric irregular particles by developing the four boundary condition equations into 4L equations that may be solved numerically for the expansion coefficients to arbitrary accuracy. In Section IV, comparisons with exact calculations for spheres and ellipsoids of revolution¹² are presented and the computation problems for more general particles are discussed. The effects of irregularity on the scattering phase functions for single particles are reviewed, and calculations performed for comparison with Reference (7) are presented and discussed.

II. PRELIMINARY

The Hertz vectors Π and Ξ are related to the electric and

SEARCHED	INDEXED	SERIALIZED	FILED
Pex Basic ref			
F. ASC Vol. I			
CONTINUATION/AVAILABILITY UNIT			
AIRL. OR/IN FORM			
A			

78 06 12 028

FOWLER

magnetic fields \vec{E} and \vec{H} by⁹

$$\vec{E} = ik\nabla \times \vec{\Pi} + k^2 m^2 \vec{\Sigma} + \nabla(\nabla \cdot \vec{\Sigma}) \quad (1)$$

and

$$\vec{H} = k^2 m^2 \vec{\Pi} + \nabla(\nabla \cdot \vec{\Pi}) - ikm^2 \nabla \times \vec{\Sigma} \quad (2)$$

where m^2 , the square of the complex refractive index is

$$m^2 = \epsilon + 4\pi i\sigma/\omega \quad (3)$$

ϵ is the dielectric constant, σ is the conductivity, ω is the radial frequency, k is the wave number of the monochromatic incident light, and $\omega = ck$ (c = speed of light.)

The requirement that \vec{E} and \vec{H} be transverse as $r \rightarrow \infty$ (the far field)², implies that only the radial components of $\vec{\Pi}$ and $\vec{\Sigma}$ need be considered,

$$\vec{\Pi} = \hat{r}\pi \quad (4)$$

$$\vec{\Sigma} = \hat{r}\sigma \quad (5)$$

where \hat{r} is the radial unit vector, and π and σ are known as Debye potentials.⁹ The vector wave equation satisfied by π and σ reduces to a scalar equation

$$(\nabla^2 + k^2 m^2) \begin{pmatrix} \pi \\ \sigma \end{pmatrix} = 0 \quad (6)$$

Equations (1), (2), (4), and (5) may be used to write the components of \vec{E} and \vec{H} in terms of the Debye potentials as

$$E_r = k^2 m^2 \sigma + \frac{\partial^2 \sigma}{\partial r^2} \quad (7)$$

$$E_\theta = \frac{ik}{r \sin(\theta)} \frac{\partial \pi}{\partial \phi} + \frac{1}{r} \frac{\partial^2 \sigma}{\partial \theta \partial r} \quad (8)$$

$$E_\phi = -\frac{ik}{r} \frac{\partial \pi}{\partial \theta} + \frac{1}{r \sin(\theta)} \frac{\partial^2 \sigma}{\partial \phi \partial r} \quad (9)$$

$$H_r = k^2 m^2 \pi + \frac{\partial^2 \pi}{\partial r^2} \quad (10)$$

$$H_\theta = \frac{1}{r} \frac{\partial^2 \pi}{\partial \theta \partial r} - \frac{ik}{r \sin(\theta)} \frac{\partial \sigma}{\partial \phi} \quad (11)$$

$$H_\phi = \frac{1}{r \sin(\theta)} \frac{\partial^2 \pi}{\partial \phi \partial r} + \frac{ikm^2}{r} \frac{\partial \sigma}{\partial \theta} \quad (12)$$

FOWLER

If the incident light is a plane wave propagating along the z axis, then

$$E_x = \exp(ikz) \quad (13)$$

$$H_y = i \exp(ikz) \quad (14)$$

which give rise to Debye potentials of the form

$$\sigma_i = k^{-2} \sum_{\ell} i^{\ell-1} \frac{2\ell+1}{\ell(\ell+1)} \psi_{\ell}(kr) P_{\ell}^1(\cos\theta) \begin{pmatrix} \cos(\phi) \\ \sin(\phi) \end{pmatrix} \quad (15)$$

where the superscript "i" indicates the incident wave. The general solution of Equation (6) has the form

$$S = \sum_{\ell, m} \{ \alpha_{\ell} \psi_{\ell}(kmr) + \beta_{\ell} \eta_{\ell}(kmr) \} P_{\ell}^m(\cos\theta) \{ \gamma_m \sin(m\phi) + \delta_m \cos(m\phi) \} \quad (16)$$

where $\psi_{\ell}(x) = x j_{\ell}(x)$, $\eta_{\ell}(x) = x y_{\ell}(x)$, $j_{\ell}(x)$ and $y_{\ell}(x)$ are spherical Bessel functions and P_{ℓ} is the ℓ th Legendre polynomial of order ℓ . The interior ("w") and scattered ("s") potentials may be written from Eq. (16) by noting from Eq. (15) that only $m=1$ terms will appear. Further, the interior potentials must converge to zero as $r \rightarrow 0$ so that $\beta_{\ell} = 0$, and the scattered potentials must converge to spherical waves as $r \rightarrow \infty$, so that $\beta_{\ell} = i \alpha_{\ell}$. This latter condition is equivalent to replacing ψ and η with $g_{\ell} = x h_{\ell}$, where h_{ℓ} is the spherical Hankel function of the first kind. These potentials may be written as

$$\sigma_w = k^{-2} \sum_{\ell} \begin{pmatrix} a_{\ell} \cos(\phi) / m^2 \\ b_{\ell} \sin(\phi) / m \end{pmatrix} \psi_{\ell}(kmr) P_{\ell}^1(\cos\theta) \quad (17)$$

$$\sigma_s = k^{-2} \sum_{\ell} \begin{pmatrix} c_{\ell} \cos(\phi) \\ d_{\ell} \sin(\phi) \end{pmatrix} \rho_{\ell}(kr) P_{\ell}^1(\cos\theta) \quad (18)$$

For a sphere, the transverse continuity boundary condition⁴ requires that E_{θ} , E_{ϕ} , H_{θ} , and H_{ϕ} be continuous across the boundary of the sphere. Inspection of Eqs. (7)-(12) reveals that this boundary condition will be satisfied if

$$\frac{\partial}{\partial r} (\sigma^i + \sigma^s) \Big|_{r=a} = \frac{\partial}{\partial r} \sigma^w \Big|_{r=a} \quad (19)$$

$$\frac{\partial}{\partial r} (\pi^i + \pi^s) \Big|_{r=a} = \frac{\partial}{\partial r} \pi^w \Big|_{r=a} \quad (20)$$

$$(\sigma^i + \sigma^s)|_{r=a} = m^2 \sigma^w|_{r=a} \quad (21)$$

$$(\pi^i + \pi^s)|_{r=a} = \pi^w|_{r=a} \quad (22)$$

where a is the radius of the sphere. Equations (19)-(22) may be reduced by using the orthogonality of the P_ℓ^1 , $\cos(\phi)$, and $\sin(\phi)$ and the explicit forms of the Debye potentials to

$$i^{\ell-1} \frac{2\ell+1}{\ell(\ell+1)} \psi_\ell'(ka) + c_\ell \rho_\ell^1(ka) = \frac{1}{m} a_\ell \psi_\ell'(kma) \quad (23)$$

$$i^{\ell-1} \frac{2\ell+1}{\ell(\ell+1)} \psi_\ell'(ka) + d_\ell \rho_\ell^1(ka) = b_\ell \psi_\ell'(kma) \quad (24)$$

$$i^{\ell-1} \frac{2\ell+1}{\ell(\ell+1)} \psi_\ell(ka) + c_\ell \rho_\ell^1(ka) = a_\ell \psi_\ell(kma) \quad (25)$$

$$i^{\ell-1} \frac{2\ell+1}{\ell(\ell+1)} \psi_\ell(ka) + d_\ell \rho_\ell^1(ka) = \frac{1}{m} b_\ell \psi_\ell(kma) \quad (26)$$

where $\psi_\ell'(x) = \partial \psi_\ell(x) / \partial x$. Equations (23)-(26) are commonly solved for c_ℓ and d_ℓ and are called the Mie solution. These c_ℓ and d_ℓ are then used to calculate the cross sections and phase functions.

III. CALCULATIONS

The radius of an irregular, but cylindrically symmetric particle may be defined by

$$r = \sum_{n=1}^{\infty} s_n P_n(\cos \theta) \equiv a(\theta). \quad (27)$$

The normal vector to the surface is

$$\hat{n} = \frac{\hat{r} - \hat{\theta} \partial \ln(a(\theta)) / \partial \theta}{1 + \left(\frac{\partial \ln(a(\theta))}{\partial \theta} \right)^2}. \quad (28)$$

The boundary conditions are

$$\hat{n} \times \Delta E|_{r=a(\theta)} = 0 \quad (29)$$

$$\hat{n} \times \Delta \mathbf{H} \Big|_{r=a(\theta)} = 0 \quad (30)$$

where

$$\Delta \mathbf{E} = \mathbf{E}^i + \mathbf{E}^s - \mathbf{E}^w \quad (31)$$

$$\Delta \mathbf{H} = \mathbf{H}^i + \mathbf{H}^s - \mathbf{H}^w. \quad (32)$$

These boundary conditions may be explicitly written as

$$\Delta E_\phi = 0 \quad (33)$$

$$\Delta H_\phi = 0 \quad (34)$$

$$\Delta E_\theta - \frac{\partial \ln a(\theta)}{\partial \theta} \Delta E_r = 0 \quad (35)$$

$$\Delta H_\theta - \frac{\partial \ln a(\theta)}{\partial \theta} \Delta H_r = 0. \quad (36)$$

Equations (33)-(36) differ from the Mie boundary conditions only in the ΔE_r and ΔH_r terms in Eqs. (35) and (36) that arise from the non spherical nature of the particle. These equations cannot be simplified in the same manner as the Mie solution by exploiting the orthogonality of the angular functions because the radius of the particle is itself a function of angle θ . Equations (31) and (32) may be used to rewrite Eqs. (33)-(36) as

$$E_\phi^s - E_\phi^w = -E_\phi^i \quad (37)$$

$$H_\phi^s - H_\phi^w = -H_\phi^i \quad (38)$$

$$E_\theta^s - E_\theta^w - \frac{\partial \ln a(\theta)}{\partial \theta} (E_r^s - E_r^w) = -E_\theta^i + \frac{\partial \ln a(\theta)}{\partial \theta} E_r^i \quad (39)$$

$$H_\theta^s - H_\theta^w - \frac{\partial \ln a(\theta)}{\partial \theta} (H_r^s - H_r^w) = -H_\theta^i + \frac{\partial \ln a(\theta)}{\partial \theta} H_r^i \quad (40)$$

The individual components of the electric and magnetic fields may be calculated in terms of the Debye potentials by use of Eqs. (7)-(12) and substituted into Eqs. (37)-(40). These resulting equations are functions only of the angles θ and ϕ , incorporating 4L unknowns; a_ℓ , b_ℓ , $c_{\ell,1}$ and d_ℓ . By calculating the overlap of Eqs. (37) and (39) with $P_\ell^1(\cos\theta) \cos(\phi)$ and Eqs. (38) and (40) with $P_\ell^1(\cos\theta) \sin(\phi)$, 4L equations in 4L unknowns may be formed. It may be noted that the ϕ integrations may be performed immediately. The resulting 4L

FOWLER

equations may be expressed in figurative form as

$$\sum_{l=1}^L B_{ll'} G_l = \sum_{l=1}^L F_{l'l'} \quad (41)$$

where

$$B = \begin{pmatrix} A_{ll',10} & -iA_{ll',9} & -A_{ll',15} & -iA_{ll',14} \\ -imA_{ll',9} & -mA_{ll',10} & iA_{ll',14} & A_{ll',15} \\ -(A_{ll',6} + A_{ll',8}) & -iA_{ll',7} & (A_{ll',11} + A_{ll',13}) & iA_{ll',12} \\ -imA_{ll',7} & -m(A_{ll',6} + A_{ll',8}) & iA_{ll',12} & (A_{ll',11} + A_{ll',13}) \end{pmatrix} \quad (42)$$

$$G = \begin{pmatrix} a_l \\ b_l \\ c_l \\ d_l \end{pmatrix} \quad (43)$$

and

$$F = \begin{pmatrix} (iA_{ll',4} + A_{ll',5}) \\ - (iA_{ll',4} + A_{ll',5}) \\ - (A_{ll',1} + iA_{ll',2} + A_{ll',3}) \\ - (A_{ll',1} + iA_{ll',2} + A_{ll',3}) \end{pmatrix} \quad (44)$$

Each element $A_{ll',n}$ is an L by L array whose entries are the integrals given for $n = 1, 6, 11$ (by steps of five) by

$$A_{ll',n} = \int f_n(a(\theta)) \frac{\partial \ln a(\theta)}{\partial \theta} P_l^1(\cos \theta) P_{l'}^1(\cos \theta) d\cos \theta \quad (45)$$

where

$$f_1 = i^{l-1} \frac{2l+1}{l(l+1)} \{ \psi_l(ka) + \psi_l''(ka) \}$$

$$f_6 = \{\psi_\ell(kna) + \psi_\ell''(kna)\} \quad (46)$$

$$f_{11} = \{\rho_\ell^1(ka) + \rho_\ell^{1''}(ka)\}$$

and

$$A_{\ell\ell',n+1} = \int g_n P_\ell^1 P_{\ell'}^1 \frac{d\cos\theta}{\sin(\theta)} \quad (47)$$

$$A_{\ell\ell',n+2} = \int g_n \frac{\partial}{\partial\theta} P_\ell^1 P_{\ell'}^1 \frac{d\cos\theta}{ka(\theta)} \quad (48)$$

$$A_{\ell\ell',n+3} = \int g_n \frac{\partial}{\partial\theta} P_\ell^1 P_{\ell'}^1 \frac{d\cos\theta}{ka(\theta)} \quad (49)$$

$$A_{\ell\ell',n+4} = \int g_n P_\ell^1 P_{\ell'}^1 \frac{d\cos\theta}{\sin(\theta)} \quad (50)$$

where

$$g_1 = i^{\ell-1} \frac{2\ell+1}{\ell(\ell+1)} \psi_\ell(ka)$$

$$g_6 = \psi_\ell(kna)/m \quad (51)$$

$$g_{11} = \rho_\ell^1(ka).$$

Equation (41) may be solved numerically for the a_ℓ , b_ℓ , c_ℓ , and d_ℓ , and the cross sections and phase functions may be calculated from the c_ℓ and d_ℓ using the same formulas as before.

IV. CALCULATIONS

A computer code was generated to perform the calculations described in the previous section. The integrals $A_{\ell\ell',n}$ Eqs. (45)-(51), were performed using a Gauss-Legendre Quadrature.¹³ Equation (41) was solved using a Gauss-Jordan elimination routine modified to treat complex entries.^{13,14} The cross sections and phase functions were calculated in the usual manner.^{15,16}

The theoretical development advanced in Section II is, of course, also valid for particles not cylindrically symmetric with respect to the incident plane wave. At this time, however, an extension of the theory and the computer code to consider these more general geometries is not feasible due to computer limitations. If a general particle or incident direction were to be considered, Eqs. (17) and (18) would include terms $\cos(m\phi)$ and $\sin(m\phi)$, $m = 0$ to L . The size of the array B would increase to approximately $4L^2$ by $4L^2$ since each current entry would increase by terms m and m' . Arrays G and F would increase in size from $4L$ to $4L^2$. Thus the total storage required would increase from $16L^2 + 8L$ to $16L^4 + 8L^2$. For $L^4 \gg L^2 \gg L$,

this is an approximate increase by a factor of L^2 . The increase in computer memory required for operational code (as compared to array storage) should be approximately proportional. The present code requires 2×8^5 words to initiate compilation, so that $L^2 \approx 8^4$ words and a general code will require approximately 2×8^9 words to initiate compilation. Computer memory of this extent is available only on a very few machines so that the implementation is not feasible at this time.

It should be noted that while this code requires a large amount of computer memory for initial compilation (2×8^5 words,) this does not restrict the utility of the code as much as might be expected. This code is normally exercised on the MICOM CDC 6600 computer using the SCOPE 3.4.2 compiler. This is a two pass compiler that performs some optimization of the compiled code. In this case, the optimization is significant as the computer memory required for the compiled code is only 6.5×8^4 words. Additionally, execution of the code is accomplished in about 15 seconds for a nominal particle of up to 19 terms in the radius (Eq.(17) and (18)) and Mie parameter of value nine, although compilation of the code requires about 60 seconds. Thus, the compiled code may be used to perform calculations with only moderate demands on computer memory and execution time in contrast to recompilation of the code for each particle to be considered.

The code was checked by exercising it for various sizes of spherical particles and various complex refractive indices. These results (c_ℓ, d_ℓ , cross sections and phase functions) were compared with the equivalent quantities calculated using a standard Mie code.¹⁷ The c_ℓ and d_ℓ for all calculations agreed to within the round-off error of the machine (fifteenth figure.)

An additional check was made by making calculations for prolate spheroids of semimajor to semiminor axis ratio of two. These calculations were compared with exact calculations.¹² There were minor differences between the approximate calculations of this paper and the exact calculations in terms of the fine structure of the phase functions, but the positions of relative maxima and minima and the relative magnitude of the curves agreed very well. These calculated phase functions are shown in Figure (1). While a precise estimate of accuracy is difficult, a comparison of calculated values with values from the exact curves at 10^0 increments gave an error bound of $\pm 2\%$ for value of $c = 2\pi a \sqrt{.75}/\lambda = 1, 3, 5, 7$ (a = semimajor axis) with an average error of approximately $8 \times 10^{-2} \%$. Because some of this error may be attributed to computer noise and the truncation error of the Gauss-Legendre integration, this error bound seems to be reasonable. The agreement shows that the code is useful despite the assumption of the validity of the Rayleigh Hypothesis.

The modification to Mie theory advanced by Chylek et al.

was examined.⁷ In this modification, based on the consideration that glories are not observed in experimental data, the particle irregularity is modeled by truncation of the resonances in the c_ℓ and d_ℓ in the region $2\pi r/\lambda = \ell$ when $\ell > 3$ in a standard Mie code. While this modification is attractive because it offers a simple, efficient computational treatment of non spherical particle scattering, the validity of the approximation has been questioned.¹⁸

As a starting point in considering the Chylek et al. modification, the cross sections and phase functions for several variations of particle size and shape were calculated. In terms of the Mie parameter,

$$x_0 = 2\pi r/\lambda, \quad (52)$$

particles of shape function

$$x(\theta) = x_0 \{1 \pm .1 P_n(\theta)\} \quad (53)$$

for $x_0 = 1, 3, 5, 7, 9$ and $n = 2, 3, 4$ were considered. A refractive index of $1.5 + 0i$ was used in this and all subsequent calculations. Cross sections both greater than and less than the equivalent Mie cross sections for the same value of x_0 were observed. The forward scatter and backscatter varied similarly, in some cases being greater and in other less. The structure of the phase functions were similar but not identical to the Mie phase functions. Although it is difficult to draw concise trends, it was noted that in general differences increased with increasing n and decreased with increasing x_0 .

Additionally, the effect of varying the strength of the deformation was examined. Shape functions of the form

$$x(\theta) = x_0 \{1 \pm a_n P_n(\theta)\} \quad (54)$$

for $n = 2$ and 3 , $a_n = .05, .1$, and $.15$ were considered. Two effects of this variation of a_n were noted; the values of the relative maxima and minima varied by as much as a factor of five although the positions of the maxima and minima varied only slightly, and the amount of near forward scattering (scattering angle less than 30°) varied by as much as a factor of five about the equivalent Mie curve. This latter effect would seem significant in terms of the experimental data reported by Chylek et al. The significance of the other effects is more difficult to assess due to the averaging process performed when the polydisperse phase functions are calculated.

The behavior of the c_ℓ and d_ℓ in the region $x_0 \approx \ell$ was studied to examine the validity of the modification of Chylek et al. Shape function of the form of Eq. (53) for $x_0 = 3$ to 4.5 by steps of $.1$, and $n = 2, 3, 4, 5$ were considered. The real and imaginary parts of c_3 and d_3 were compared with the c_3 and d_3 calculated using Mie theory. In seven of these eight calculations, the resonance curve shape is

FOWLER

preserved although it narrows by as much as a factor of two. Additionally, the center of the resonance curve shifts, apparently without trend, although the resonance curves (real parts) for the irregular particles always fall under the Mie resonance curves. In one case, that of $x(\theta) = x_0\{1 + .1P_3(\theta)\}$, the resonance curve is replaced by a slowly varying curve contained under the Mie curve (real part) whose real parts have a mean of approximately .3 and whose imaginary parts have a mean of approximately zero. In all other cases, the resonance curves narrow and fall under the Mie curves. The extent of narrowing appears to be approximately proportional to n . On the basis of these calculations, the modification of the c_ℓ and d_ℓ in the resonance region is not substantiated, but the numerical results of Reference (7) might be justified in view of the narrowing of the resonance curves.

Calculations were also performed for one of the polydisperse aerosol distributions reported by Chylek et al. (i.e. the first KCl.) Nine phase functions using

$$\begin{aligned} x(\theta) &= x_0 \\ x(\theta) &= x_0\{1 \pm .05 P_2(\theta)\} \\ x(\theta) &= x_0\{1 \pm .1 P_2(\theta)\} \\ x(\theta) &= x_0\{1 \pm .15 P_2(\theta)\} \\ x(\theta) &= x_0\{1 - .1 P_2(\theta) \pm .1 P_4(\theta)\} \end{aligned}$$

were calculated and combined linearly with adjustable coefficients calculated using regression techniques to fit the data. Two different fitting techniques were used; one using all the data, and another using only those data for scattering angles greater than sixty degrees. A representative fit for each scheme is shown in Figure (2). These fits appear to be as good as that reported by Chylek et al. It is noted that the fit is not sensitive to the choice of combinations of phase functions used.

The insensitivity of the fits to variation in the phase functions used in the fitting calculations seems to indicate that a more elaborate calculation for more irregular shaped particles averaged over orientations would not significantly improve the results in terms of the cost of such a calculation. In the same vein, the Chylek et al. modification seems to be adequate for many calculations. It appears that more accurate calculations should be necessary for aerosols with much less random shape and orientation.

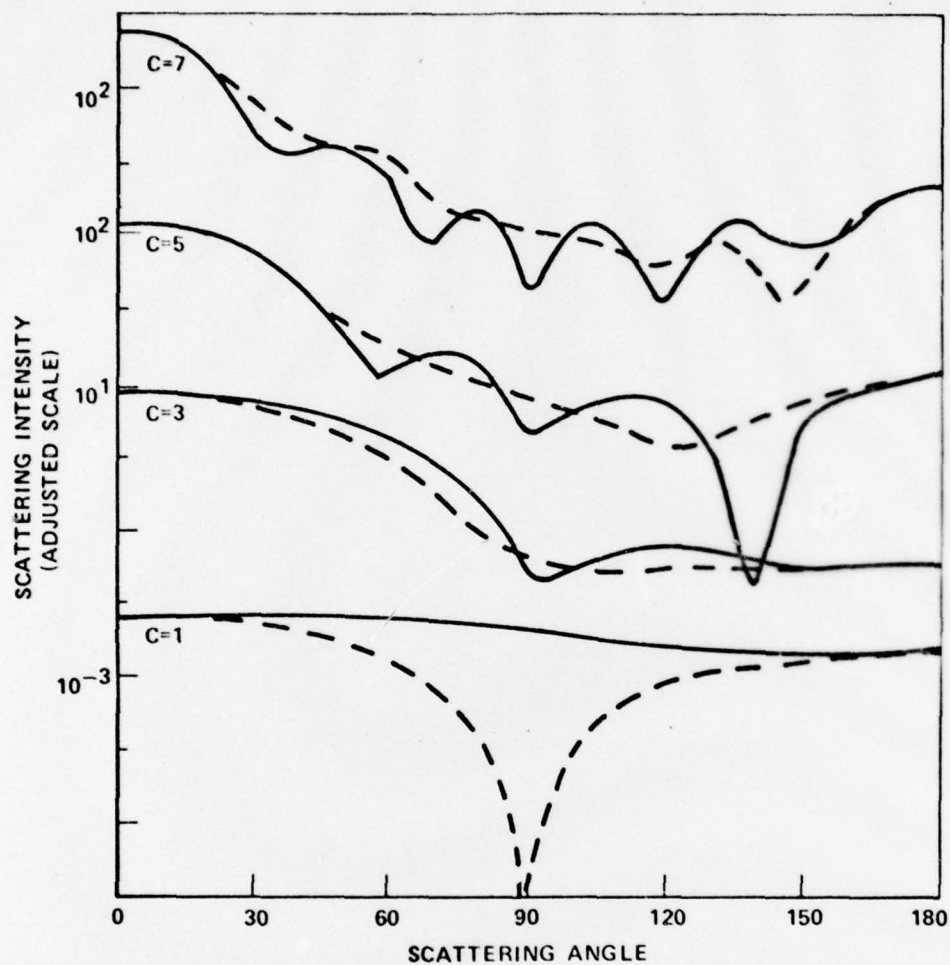


Figure (1). Calculated phase functions for prolate spheroids used for comparison with the exact phase function of Reference (12).

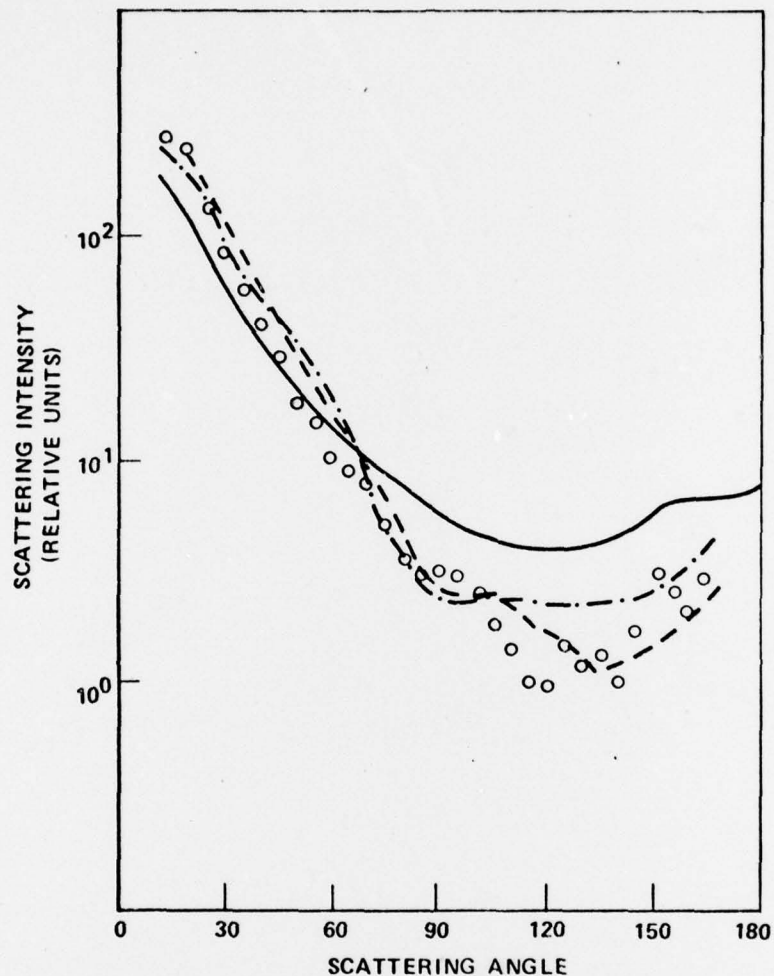


Figure (2). Comparison of non spherical experimental data (circles) with figurative Mie phase function (solid curve) and two composite non spherical phase functions (dashed curves.) The dashed curve is fitted over all data, and the dashed-dotted curve is fitted only over data for scattering angle greater than sixty degrees. Phase functions for shape functions incorporating $-.05$, $-.1$, and $-.15 P_2(\theta)$ were used in this fit.

FOWLER

REFERENCES

1. Fowler, B. W., and C. C. Sung, Appl. Opt., to be published circa July, 1978.
2. Millar, R. F., Radio Science, 8 785 (1971).
3. Davies, J. B., IEEE Trans. Microwave Theory, Tech., MTT-21(2) 99 (1973).
4. Eyres, L., and A. Nelson, Ann. Phys., 100 37 (1976).
5. Uzunoglu, U. K., and A. R. Holt, J. Phys. A., 10 413 (1973).
6. Waterman, U. K., Phys. Rev., D3 825 (1971).
7. Chylek, P., G. W. Grams, and R. G. Pinnick, Science, 193 480 (1976).
8. Mie, G., Ann. D. Physik. (4), 25 377 (1908).
9. Born, M. and E. Wolf, Principles of Optics, Pergamon Press, Oxford, 1975.
10. Schiff, L. I. Quantum Mechanics, McGraw Hill, New York, 1968.
11. Ward, G., "Scattering of Electromagnetic Radiation from Irregular dielectric Particles", unpublished.
12. Asano, S. and C. Yamamoto, Appl. Opt., 14 29 (1975).
13. Carnahan, B., H. A. Luther, and J. C. Wilkes, Applied Numerical methods, John Wiley and Sons, Inc., New York, 1969.
14. Sellers, W. R., and B. G. Gibbs, Descriptions-General Purpose Computer Subroutines, US Army Missile Command Report No. TR-WS-75-2, January 1977.
15. Van de Hulst, H. C., Light Scattering by Small Particles, John Wiley and Sons, Inc. New York, 1957.
16. Biermendjian, D., Electromagnetic Scattering on Spherical Polydispersions, Elsevier, New York, 1964.
17. Blattner, W., Utilization Instructions for Operation of the Mie Programs on the CDC-6600 at AFCRL, Research Note RRA-N7240, contract F19628-70-c-0156, Radiation Research Associates, Inc., 1972.

FOWLER

18. Kerker, M., private communication, 1977.